CONF-940553--93

SIMULATION OF FLOW IN THE UNSATURATED ZONE BENEATH PAGANY WASH, YUCCA MOUNTAIN

Edward M. Kwicklis
U.S Geological Survey
Box 25046, M.S. 421
Denver Federal Center
Lakewood, CO 80225
(303) 236-6228

Alan L. Flint
U.S. Geological Survey
P.O. Box 327,M.S. 721, Area 25
Hydrologic Reseach Facility
Mercury, NV 89023 Bldg. 4215
(702) 295-5805

Richard W. Healy
U.S. Geological Survey
Box 25046, M.S. 413
Denver Federal Center
Lakewood, CO 80225
(303) 236-5392

ABSTRACT

A one-dimensional numerical model was created to simulate water movement beneath Pagany Wash, Yucca Mountain, Nevada. Model stratigraphy and properties were based on data obtained from boreholes UE-25 UZ #4 and UE-25 UZ #5, which were drilled in the alluvial channel and bedrock sideslope of Pagany Wash. Although unable to account for multidimensional or preferential flowpaths beneath the wash, the model proved a useful conceptual tool with which to develop hypotheses and, in some cases, provide bounding calculations. The model indicated that liquid flux decreases with depth in the upper 120 m beneath the wash, with fluxes of several tens mm/yr in the nonwelded base of the Tiva Canyon Member and fluxes on the order of a tenth mm/yr in the upper Topopah Spring Member. Capillary barrier effects were indicated by the model to significantly delay the entry of large fluxes into the potential repository horizon during periods of increasing net infiltration, and to inhibit rapid drainage of water from the nonwelded and bedded intervals into the potential repository horizon during periods of moisture redistribution. Lateral moisture redistribution can be expected to be promoted by these effects.

I. INTRODUCTION

With few exceptions,[1,2] previous modeling studies of water flow within the unsaturated zone at Yucca Mountain have utilized a highly simplified stratigraphy, often consisting of no more than five stratigraphic units between the ground surface and the water table. In particular, the nonwelded and bedded tuff intervals overlying the Topopah Spring Member of the Paintbrush Tuff have frequently been considered a single homogeneous unit. Recent analyses[3] of the porosity (ϕ), saturation (S) and water potential (ψ) profiles at boreholes UE-25 UZ #4 (UZ #4) and UE-25 UZ #5 (UZ #5),[4] located within Pagany Wash (figure 1), have shown that the S distribution decreases overall with depth within these intervals, but locally appears to be inversely related to ϕ. This suggests that attempts to model the S and ψ profiles need to account for the heterogeneity reflected in the ϕ profile.

To compensate for the relative sparsity of data for unsaturated hydraulic properties at these holes, Kwicklis et al.[3] developed correlations between saturated hydraulic conductivity (K), the parameters for the unsaturated hydraulic functions of van Genuchten,[5] and ϕ. They then used the measured ϕ and S profiles at boreholes UZ #4 and UZ #5 to calculate effective hydraulic conductivity (K_e) and estimate vertical water flux. One strength in that approach was that no assumptions regarding temporal variability in

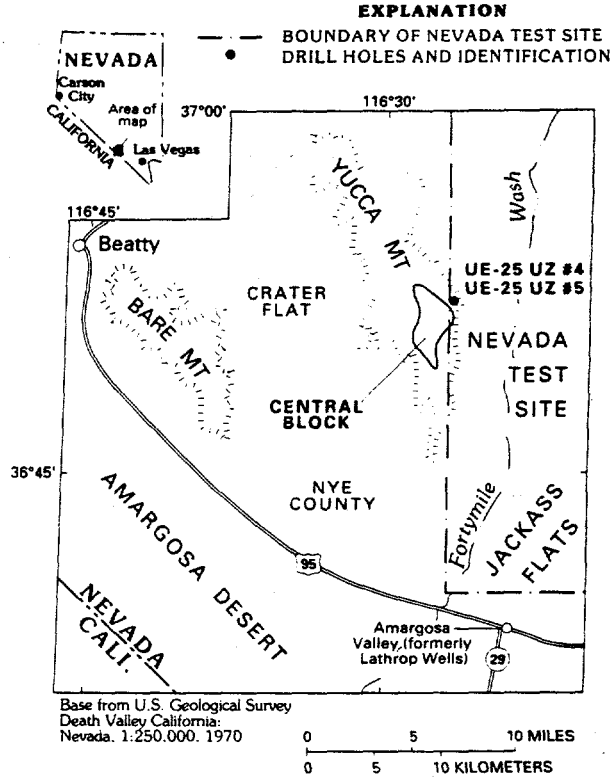

Figure 1. Location map for Pagany Wash and boreholes UZ #4 and UZ #5.

boundary conditions or dimensionality of the flow field were necessary. Their resulting water flux profiles indicated a downward flux of at least several tens of millimeters per year in the nonwelded base of the Tiva Canyon Member and the upper part of the Yucca Mountain Member. Lateral flow beneath Pagany Wash was inferred on the basis of abrupt changes in the magnitude of the downward flux at some of the bedded air-fall intervals and reversals in flow direction at the base of the Pah Canyon Member in UZ #4. Independent evidence for lateral flow in the nonwelded and bedded units underlying Pagany Wash was provided by the tritium profiles at UZ #4 and UZ #5. These profiles were characterized by multiple peaks: elevated tritium concentrations occurred within the alluvium at UZ #4, at the nonwelded base of the Tiva Canyon Member in UZ #5 and at the middle bedded interval in UZ #4.[6] The tritium peak in the base of the Tiva Canyon Member may have been associated with fracture flow through the overlying densely welded intervals. Although neutron probe measurements of moisture content over the last ten years have indicated small or negligible flux through the alluvium,[7] isotopic data have suggested that historically water fluxes have been larger than recently observed[3]. Tritium data from water samples obtained within the alluvium at UZ #4 displayed a local peak at a 4.5 m depth, from which an average recharge rate of 35.1 mm/yr was inferred for the 21-year period 1963-1984. ^{14}C apparent-age dates of 1000 and 4900 years of water samples collected from depths of approximately 100 m at UZ #4 and UZ #5 were used to compute average particle velocities. These velocities, combined with an average volumetric moisture content of 0.20 between a 100 m depth and the ground surface, provided average, long-term vertical flux estimates of 20 and 4 mm/yr at UZ #4 and UZ #5.

Each of these lines of evidence is flawed in some way. The calculated flux profiles have uncertainty because effective hydraulic conductivities (K_e) used to estimate flux are themselves uncertain.[3] The significance of flux values calculated on the basis of tritium data collected from the alluvium is uncertain because it is unclear if underlying calcium carbonate-cemented layers will permit further downward water movement. Flux estimates made on the basis of the ^{14}C data were made under the assumption of vertical 1-dimensional piston flow, which may be a poor assumption since the tritium and flux profiles both indicate lateral flow may be an important component of overall moisture movement. Although these flux estimates are somewhat flawed, collectively they should raise a cautionary flag about using recent, relatively short-term observations to draw conclusions concerning the long-term role washes such as Pagany Wash may have played in infiltration processes at Yucca Mountain. Evidence for that historical role may exist in the S and ψ profiles obtained from the deeper subsurface in the nonwelded and partially welded intervals of the Tiva Canyon, Yucca Mountain, Pah Canyon and Topopah Spring Members of the Paintbrush Tuff, and the intervening bedded layers. These profiles may reflect more integrated long-term behavior than can be identified from study of inherently more transient surficial processes.

The measured S and ψ profiles at boreholes UZ #4 and UZ #5 provide a snapshot of the shallow (upper 110 m) unsaturated zone hydrologic system for a specific, although unknown, set of boundary conditions and at a specific instant in time. To examine the dynamics of water movement within the upper unsaturated zone beneath Pagany Wash over a range of possible boundary conditions and to further investigate the possible history of past water movement beneath the wash, we have created a one-dimensional numerical model that attempts to include much of the known stratigraphic variability.

Analysis of past infiltration is complicated by a number of factors, including: (1) the probability of time-varying boundary conditions; (2) uncertainty in unsaturated hydrologic properties; and (3) the probability that multidimensional flow, and possibly preferential flow along fractures or faults, has occurred. Several plausible mechanisms could explain the evidence for lateral flow

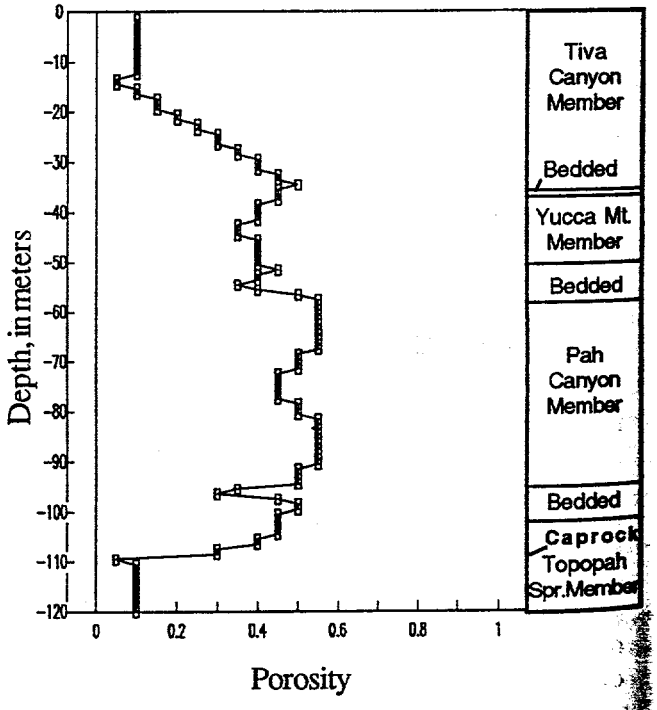

Figure 2. Porosity classes used to assign hydrologic properties.

cited above.[3,6] Water could have moved down fractures or faults and been redistributed into the adjacent rock mass to varying degrees by matrix imbibition. Northwest trending strike-slip faults have been hypothesized as controlling the location and orientation of washes, including Pagany Wash, in the northern part of Yucca Mountain.[8] Nearer to UZ #4 and UZ #5, several northeast and east trending faults intersect Pagany Wash at high angles,[8] and any of these might intercept water flowing down the wash. Infiltration into high conductivity strata where these outcrop further up the wash and water movement downdip along these layers could possibly also be responsible for the evidence indicative of lateral flow.

In the absence of detailed site-specific information about fault structures and their hydrologic characteristics, modeling of water flow beneath Pagany Wash will remain speculative. The present model also suffers from the potentially significant limitation that simulations have been completed only in one-dimension. Although this is possibly a less critical simplification when infiltration is areally widespread and diffuse, significant lateral gradients would be expected where infiltration is spatially focussed, as is suspected in the case in Pagany Wash. For these reasons, we do not present these simulation results as definitive statements regarding past water movement beneath Pagany Wash, but instead as an opportunity to develop hydrologic intuition from an idealized system that bears some resemblance to Pagany Wash. An assessment of the impact of assuming one-dimensional flow is made after presentation of the simulation results.

II. MODEL STRATIGRAPHY AND PROPERTIES

An idealized stratigraphy for the upper unsaturated zone beneath Pagany Wash was created based on measured values of ϕ from core samples taken from boreholes UZ #4 and UZ #5, and correlations previously established between K, the van Genuchten parameters (α,n) and ϕ.[3] Excluding the alluvium, combined information from boreholes UZ #4 and UZ #5 covered a stratigraphic extent of approximately 117m. Observed ϕ profiles along boreholes UZ #4 and UZ #5 were first approximated by linear interpolation. The interpolated values were then used to assign each 1-m depth interval in the upper 120 m at each hole to one of twelve ϕ classes: 0.05, 0.10, 0.15, 0.20, 0.25, 0.30, 0.35, 0.40, 0.45, 0.50, 0.55, and 0.60 (figure 2). Below a 120m depth, grid spacing approximately doubled and a uniform ϕ of 0.10 was assumed between that depth and the water table at 472m, which formed the lower boundary in the computational grid. Unsaturated hydraulic properties for each ϕ class were derived on the basis of the correlations and the nominal ϕ value. The small ϕ, densely welded intervals have been reported to be generally more fractured than the large ϕ, nonwelded units.[9] The ϕ=0.05 to ϕ=0.30 classes were therefore given fracture porosity and permeability. These quantities were calculated by assuming 3 mutually orthogonal fracture sets each with a fracture spacing of 0.1 m. Each fracture within these sets had an

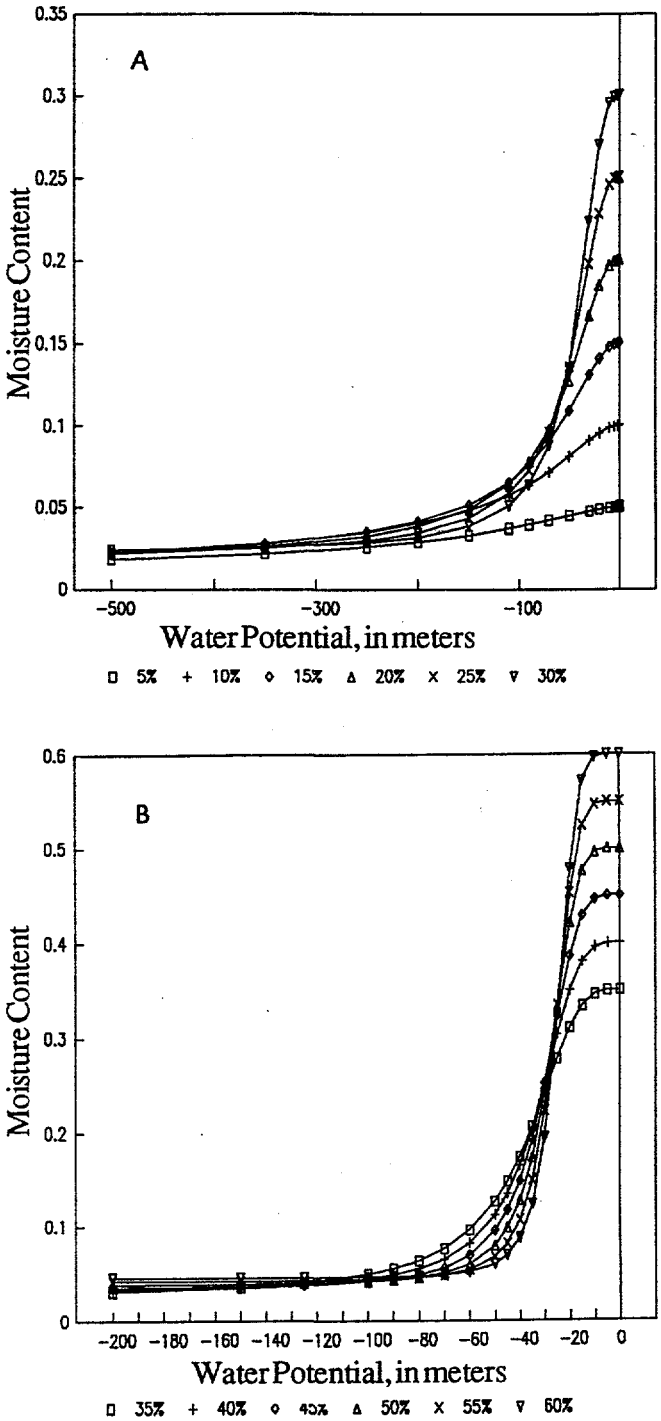

Figure 3. Moisture characteristic curves for (a) the 5 to 30% porosity classes and (b) the 35 to 60% porosity classes.

average physical aperture of 25 μm and unsaturated hydrologic properties predicted by a numerical model that considers many of the physical processes of water movement in variably saturated, rough-walled fractures.[10] The actual fracture density, as well as the physical or hydraulic apertures of fractures at these boreholes are not well characterized. However, care was taken to ensure that the transmissive and capillary properties of the fractures assumed by the model were internally consistent based on theoretical considerations. The assumption that layers with very small matrix permeability can potentially conduct large fluxes seems realistic given the reported fracture densities,[9] and one that permits a broad range of fluxes to be investigated.

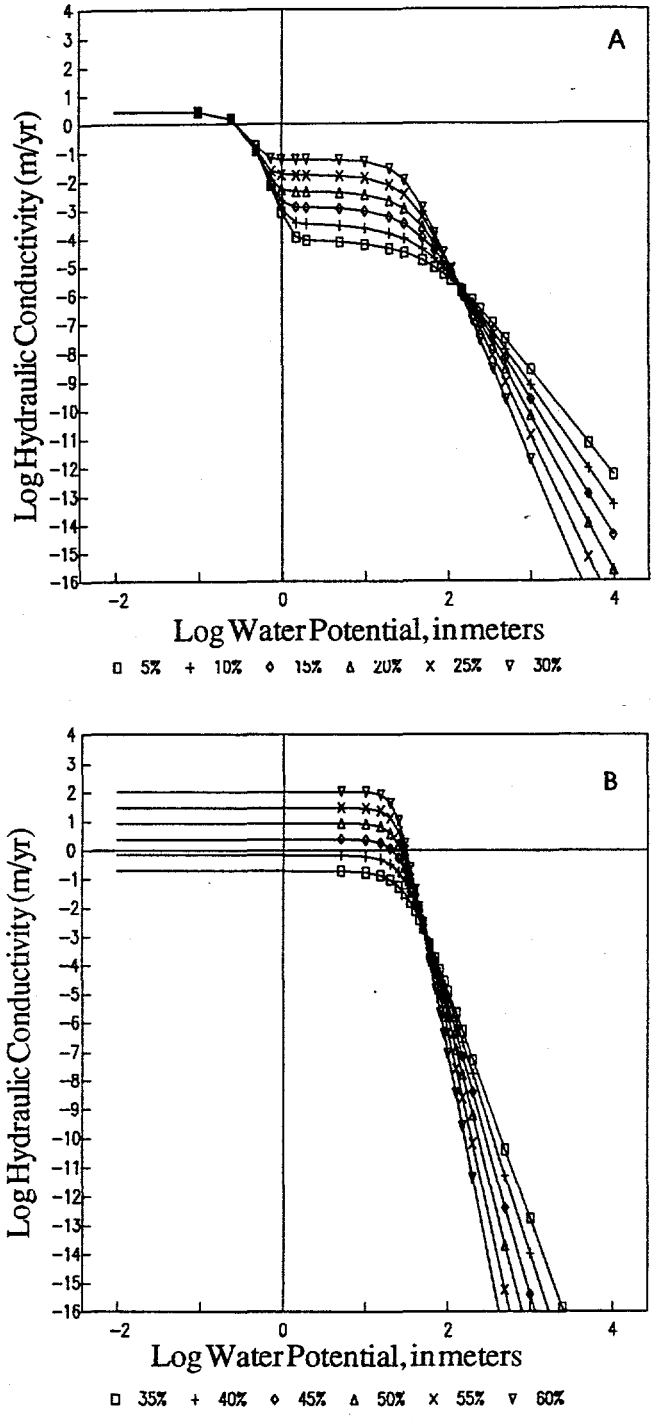

Figure 4. Log K_e versus log $|\psi|$ curves for (a) the 5 to 30% porosity classes and (b) the 35 to 60% porosity classes.

The moisture characteristic curves ($\theta(\psi)$) for the twelve ϕ classes are shown in figures 3a and 3b, and the corresponding log K_e versus log $|\psi|$ curves shown in figures 4a and 4b. These curves reflect the bulk-rock properties, including fractures, and are labeled according to matrix ϕ. In deriving these curves, matrix and fracture ψ were assumed to be equal, an assumption that allows the weighted contributions of the fracture and matrix continua to be added. In the case of the $\theta(\psi)$ curves, fracture and matrix contributions to bulk-rock θ were determined by weighting their respective saturations by ϕ; and, for the log K_e versus log $|\psi|$ curves, fracture and matrix K_e were weighted by the fractional cross-section area available to flow afforded by each continua. From figure 4a it can be seen that only when $\log|\psi|<0$ ($\psi>-1$m) do the fractures begin to contribute significantly to the overall hydraulic conductivity of the rock. All the curves in figure 4a begin to coalesce at $\log|\psi|<0$ because of the assumption of uniform fracture density and fracture properties across the 5 to 30 percent ϕ classes. The model is probably insensitive to the presence or absence of fractures in the large (>30%) ϕ classes. These are sufficiently conductive at $\psi<-1$m to transmit, under a unit gradient, the range of fluxes considered by this study. Therefore, because ψ will not exceed -1m in these ϕ classes, fracture contributions to bulk-rock K_e would have little or no effect on the results. All calculations were performed with a version of the TOUGH[11] code which was modified to accept rock hydrologic characteristics in tabular form.

Because the hydrologic properties in the present model are based on statistical relations rather than location-specific measurements, the model is perhaps a more conspicuous idealization of reality than many models. All models, however, are simplifications of the true physical system, and no single model presently accounts for all complexities that exist at the site. Even models for which numerous location-specific $\theta(\psi)$ information have been measured are currently subject to large uncertainty associated with the assumption that $K_e(\theta)$ properties can be accurately predicted from the $\theta(\psi)$ information. The present model is probably no more and possibly less an idealization than models in which a few location-specific measurements are extrapolated on the basis of either a

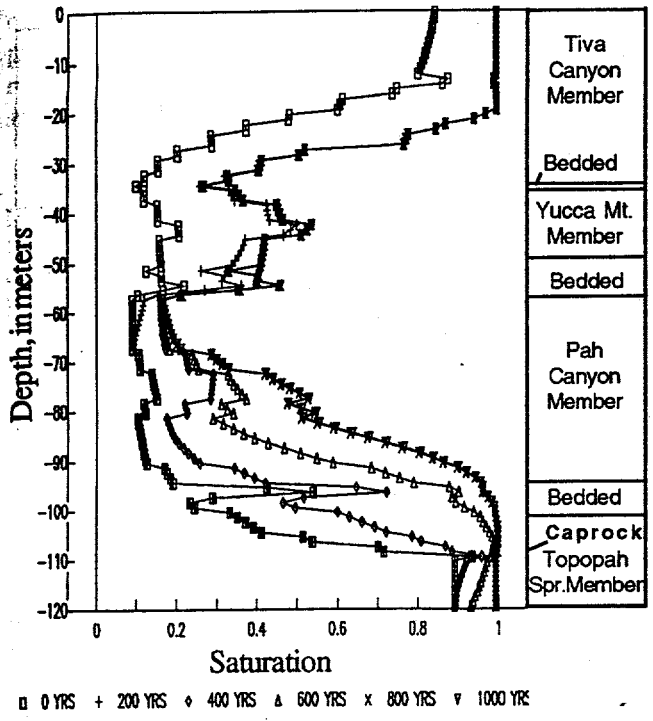

Figure 5. Evolution of the saturation profile for 1000 years following an increase in infiltration from 0.1 to 20 mm/yr.

highly simplified stratigraphy and/or similarity in the degree of welding.

III. MODEL RESULTS

A. Behavior Under Wetting Conditions

As the first step in reconstructing the infiltration history beneath the wash, simulations were run for prescribed fluxes of 0.1, 0.175, 0.25, 1.75, 10.0 and 20.0 mm/yr. The steady-state S and ψ versus depth profiles that resulted from application of these fluxes were then compared with the measured profiles at boreholes UZ #4 and UZ #5. These comparisons, made for the upper 120 m or so of the unsaturated zone, showed that the lower portion of the simulated and observed profiles appeared to be in better agreement at small fluxes (0.1 to 0.25 mm/yr), whereas the upper parts of the profiles were in better agreement at relatively large (10.0 to 20.0 mm/yr) flux values. From this finding, it was inferred that infiltration rates may have been time-varying rather than constant, with relatively larger recent values. We proceeded to explore whether a simple increase in the boundary condition from a small (0.1 or 0.175 mm/yr) to a large (10 or 20 mm/yr) flux could improve the comparison between the simulated and measured profiles. Figure 5 shows the evolution of the saturation profile for 1000 years following an instantaneous increase in infiltration from 0.1 to 20 mm/yr. Initial conditions resulted from running the model to steady state with a 0.1 mm/yr flux. After 200 years, most of the saturation changes were restricted to the lower half of the profile. Steady flow conditions within the upper 120 m were established by 800 years following the change in infiltration rate, as indicated by the similar saturation profiles at 800 and 1000 years. Based on the saturation profiles in figure 5, the saturation profile at 400 years following the infiltration increase was chosen for comparison with the measured profiles at UZ #4 and UZ #5. These comparisons are made in figure 6a for borehole UZ #4 and in figure 6b for borehole UZ #5. As a quantitative measure of the fit, root mean-square error (MSE) was calculated for the nonwelded and bedded intervals. Root MSE within these intervals was 0.180 at UZ #4 and 0.146 at borehole UZ #5.

For borehole UZ #5, the simulated profile captures not only most of the trends in the measured profile, but also does a fair job of matching the actual values. The match between the simulated and observed profiles is poorest within the Tiva Canyon Member where simulated values exceed the measured values in the densely welded intervals but underestimate the measured values in the partially and nonwelded intervals where estimates of ϕ are poorly constrained by relatively sparse data. The overestimation of S in the densely welded intervals is considered to be an acceptable error because although the model assumes that matrix and fracture flow are strongly coupled, in reality water may be moving in near surface fractures without much interaction with the adjacent matrix. If that is the case, matrix saturation in the uppermost densely welded interval would be a poor indicator of the flux through that interval. Additional discrepencies occur at the base of the profile, where some small-scale reversals in saturation trends are not well described. However, figure 6b indicates that, overall, our model, although highly idealized, is capturing many aspects of what is a fairly complex and detailed profile at UZ #5.

At UZ#4 (figure 6a), the general trends in the observed S profile are predicted fairly well, although agreement with the actual values is poorer than at UZ #5. Within the Tiva Canyon Member at UZ #4, the simulated profile again overpredicts S within the upper densely welded intervals and underpredicts S in the lower, nonwelded intervals. The discussion concerning the comparison between simulated and observed profiles within the Tiva Canyon Member at UZ #5 apply to UZ #4 as well. Unfortunately, no grain or bulk density information was reported between -86.3 and -105.7m,[4] and so neither ϕ or S could be calculated for comparison in that interval. Below -105.7m, the simulated profile consistently

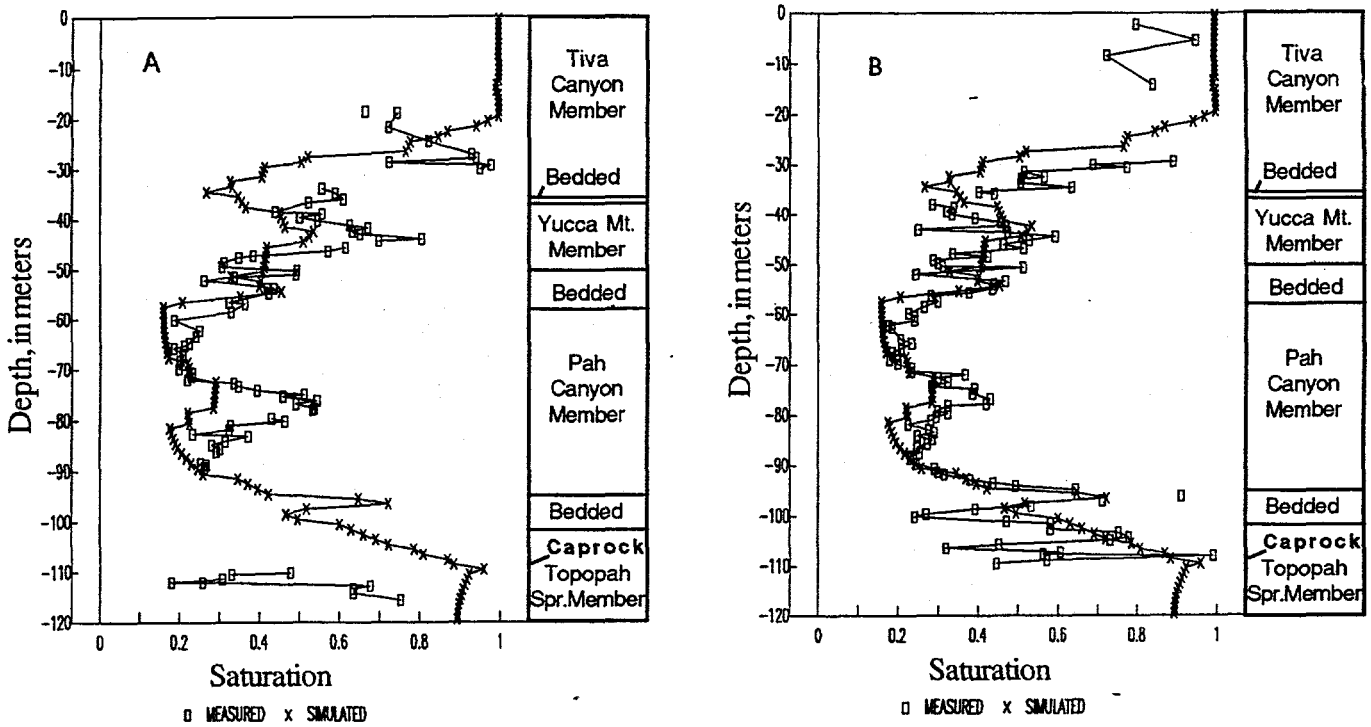

Figure 6. Comparison between the simulated saturation profile 400 years after an increase in infiltration from 0.1 to 20 mm/yr with the measured saturation profiles at (a) UZ #4 and (b) UZ #5.

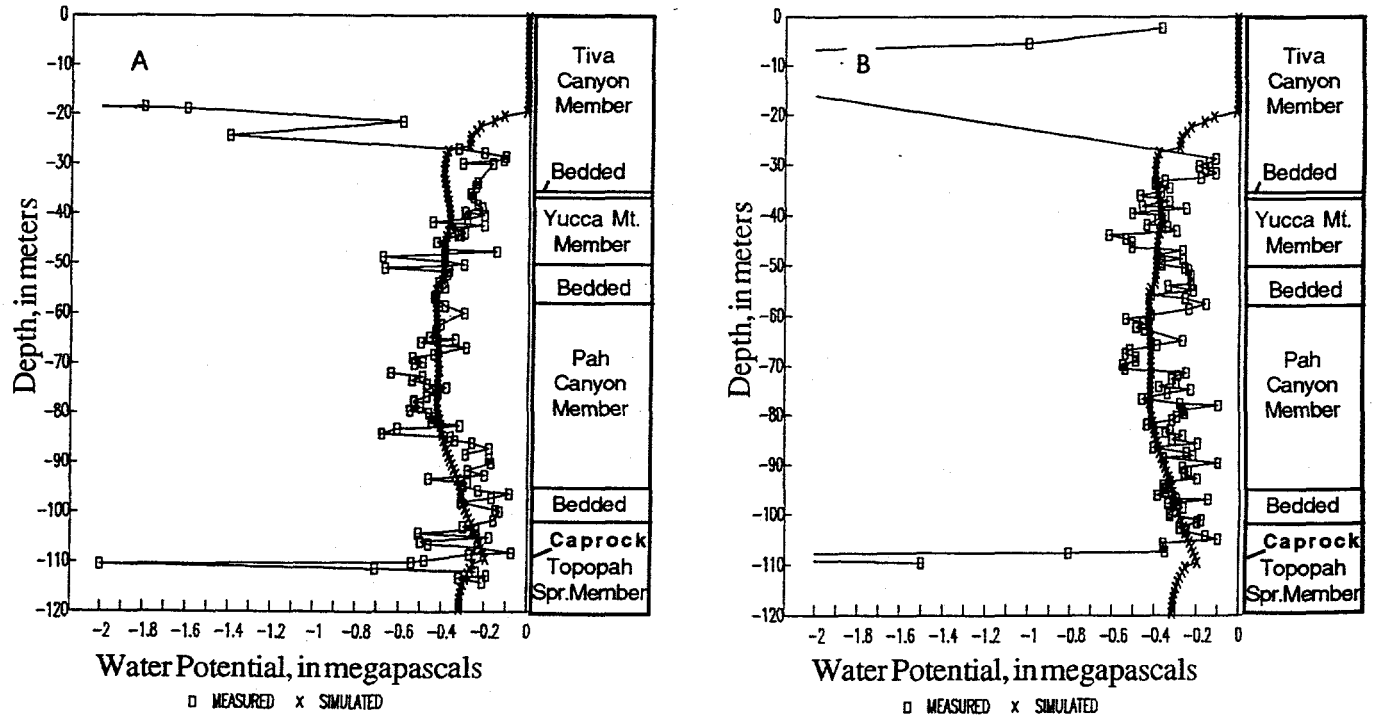

Figure 7. Comparison between the simulated water potential profile 400 years after an increase in infiltration from 0.1 to 20 mm/yr with the measured water potential profiles at (a) UZ #4 and (b) UZ #5.

overpredicts S. For reasons that are not understood at present, measured S here are very small compared with rocks of a similar degree of welding higher in the stratigraphic section.

The measured ψ at UZ #4 and UZ #5, and the ψ predicted following 400 years of infiltration at 20 mm/yr are shown in figures 7a and 7b. Measured ψ were determined by psychrometer on subsamples of core that had been taken during drilling.[4] Psychrometers actually determine the relative humidity of air in contact with the sample, from which ψ are calculated. Measurements made to infer ψ within the more densely welded intervals are suspect, because of the probability that insufficient time had been allowed to establish vapor-liquid equilibrium.[3] Within the nonwelded and partially welded zones, however, we note that many of the observed trends, as well as the actual values, are described by the simulated profiles (figures 7a and 7b). Within these intervals, root MSE values of 129.5 kPa and 127.2 kPa were calculated at UZ #4 and UZ #5. These root MSE values are only slightly greater than the inherent accuracy of the measurements themselves (about 100 kPa).[3]

Encouraged that the model appears to be capturing at least some aspects of reality, we examined the remainder (400 to 1200 years) of this simulation to observe how such a system might respond to a continued high surface flux. Figure 8a and 8b shows the relation between flux and depth for various times ranging from 100 to 1200 years after the onset of the high infiltration rate. During the time period from 100 to 400 years (figure 8a) the flux at any depth increases with time. However, from 400 to 600 years the flux profile retreats upward, indicating that flux is decreasing within the interval from approximately -80 to -110 m. Between 600 and 700 years (figure 8b) the flux profile continues to retreat upward. Finally, between 700 and 800 years the increased flux breaks through into the underlying densely welded fractured intervals of the Topopah Spring Member, and by 900 years the entire upper 120 m experiences a flux of 20 mm/yr.

During the entire period from 0 to 1200 years the surface flux has remained constant at 20 mm/yr, yet from 400 to 700 years in the simulation, flux in the 40 m or so above the vitric caprock decreased. These simulation results, which may at first seem counterintuitive, illustrate the principles of a capillary barrier. Water cannot move from the smaller openings of the overlying nonwelded units into the relatively larger openings of the fractures in the densely welded intervals, including the low ϕ vitric caprock, until ψ along the interface become sufficiently large. During the simulation period from 400 to 700 years we observed that water continues to go into storage in the interval immediately above the vitric caprock (figure 5) with a corresponding increase in ψ over the same interval (figure 9). However, it is not until 800 years that ψ within

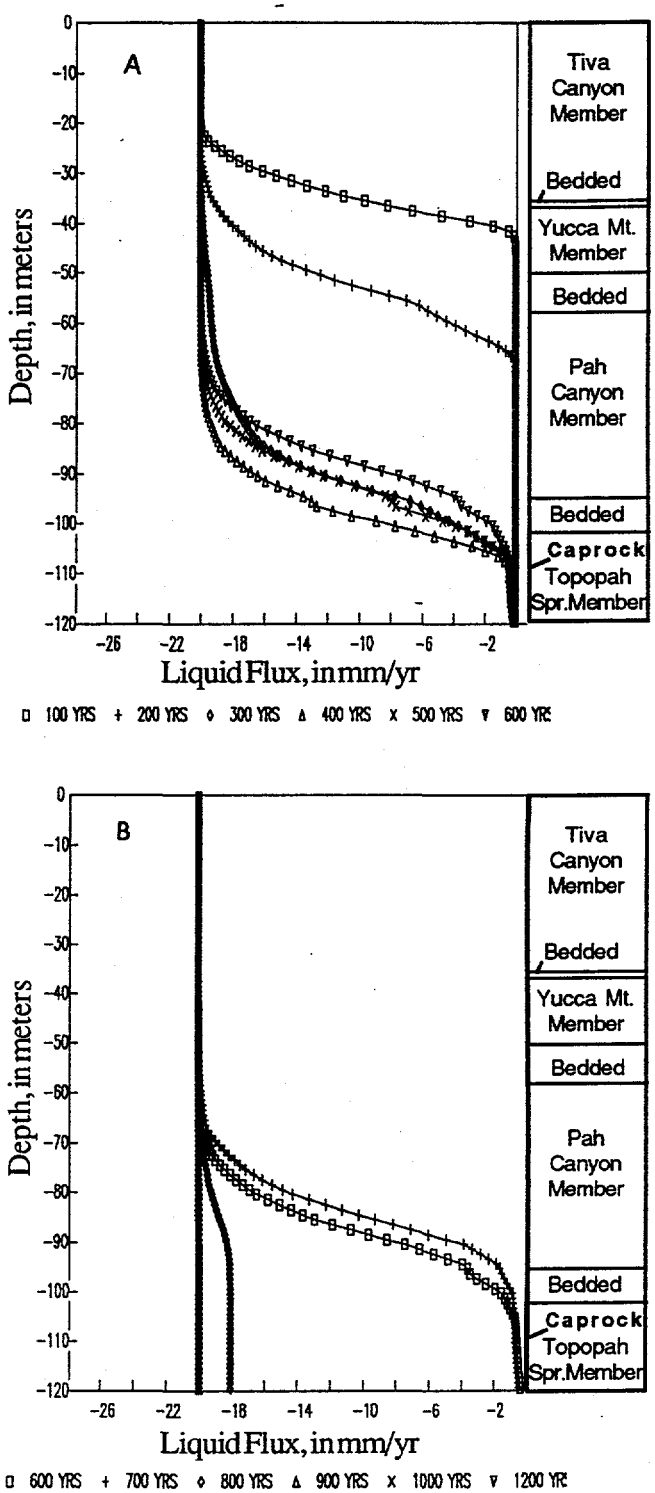

Figure 8. Evolution of the flux profile for (a) 100 to 600 years and (b) 600 to 1200 years following an increase in infiltration from 0.1 to 20 mm/yr.

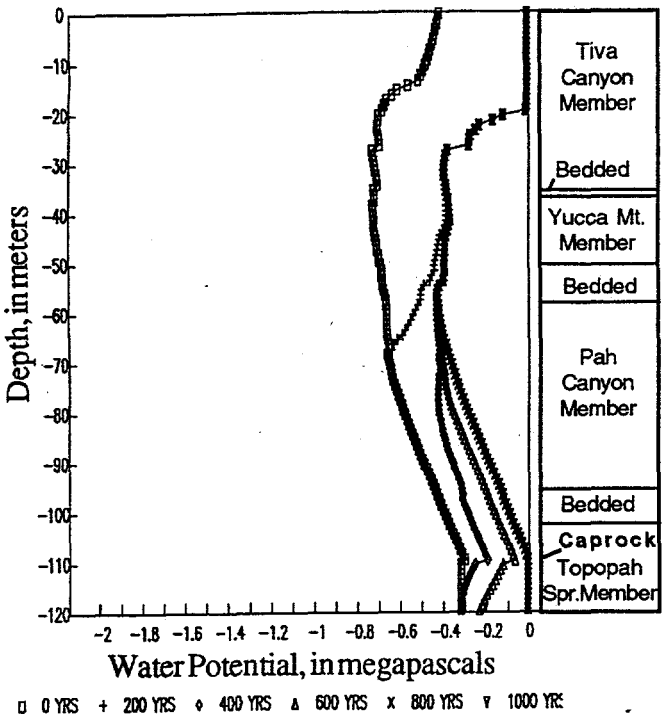

Figure 9. Evolution of the water potential profile for 1000 years following an increase in infiltration from 0.1 to 20 mm/yr.

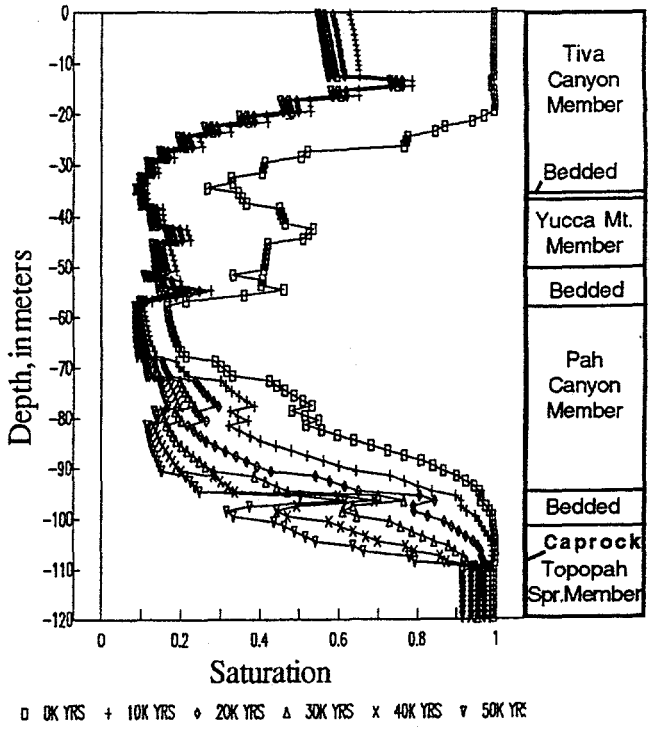

Figure 10. Evolution of the saturation profile for 50,000 years following an increase in infiltration from 0.1 to 20 mm/yr.

the vitric caprock became large enough (>-0.01MPa or -1 m) that the fractures began to transmit water at rates approaching the applied flux.

That the interface between the nonwelded and bedded units and the underlying fractured, densely welded intervals might function so effectively as a capillary barrier was not completely expected. Even if we assume that at Pagany Wash we are approximately 400 years into a period of relatively large flux (20 mm/yr), as the comparison between the measured and predicted S and ψ profiles would suggest, the simulations predict that the fluxes entering the Topopah Spring Member would remain on the order of several tenths mm/yr for at least another 300 years.

B. Behavior Under Drying Conditions

Although the relatively good match obtained previously between the observed and simulated S and ψ profiles has suggested a relatively wet recent past, we thought it would also be instructive to investigate how the system might respond during a period of moisture redistribution (with no infiltration flux) following a wet period during which a steady flow of 20 mm/yr had been established. Figure 10 shows the evolution of the saturation profile for 50,000 years following cessation of the 20 mm/yr flux and imposition of a no-flux upper boundary condition. What is most striking about this figure is that it shows that water is still draining from the upper 120 m even after 40,000 to 50,000 years. Once fractures in the vitric caprock of the Topopah Spring Member at -110 m have drained, drainage becomes exceedingly slow because water can continue to drain only through the extremely low permeability matrix. There is an extremely pronounced asymmetry in the time required to wet up the upper unsaturated zone when fracture flow is involved, and the time required to drain this same interval when drainage occurs only through a low permeability matrix. As observed in the previous section, when fluxes are large enough to initiate fracture flow, steady conditions can be established within the upper 120 m over time-scales on the order of 1000 years. We also note that none of the S profiles in figure 10 bears much resemblance to the measured profile for either UZ #4 or UZ #5, supporting our previous interpretation that the S and ψ profiles at those holes have evolved in response to relatively recent influxes of water rather than drainage from a previously wetter condition.

The ψ profiles for this 50,000 year period (figure 11)

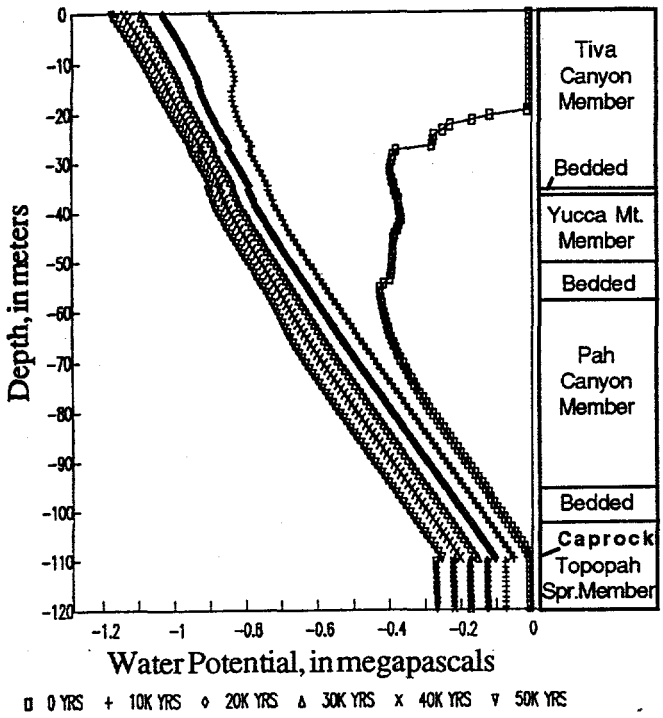

Figure 11. Evolution fo the water potential profile for 50,000 years following a change in surface infiltration from 20 to 0 mm/yr.

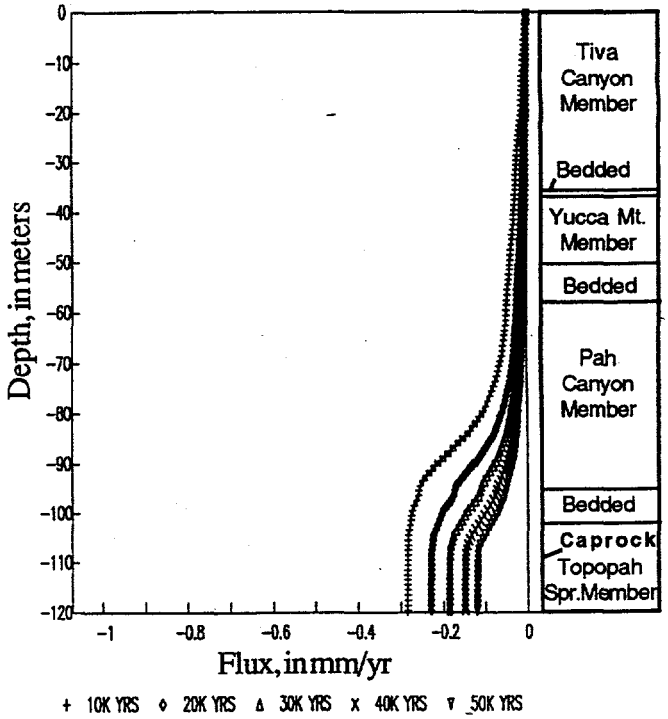

Figure 12. Evolution of the flux profile for 50,000 years following a change in surface infiltration from 20 to 0 mm/yr.

show that a condition of near-static equilibrium develops above the vitric caprock, indicative of near no-flow conditions. The profiles shift with time because drainage, although very small, is not exactly zero. The base level for this near-static equilibrium profile is the vitric caprock of the Topopah Spring Member at -110m depth, not the water table. A near-static equilibrium profile was observed in the 20 m or so above the vitric caprock at UZ #7[3]. However, the observed ψ profiles at UZ #4 and UZ #5 bear little resemblance to the predicted profiles for drainage conditions with no net infiltration.

The flux profiles for the upper 120 m during the redistribution period are shown in figure 12. These profiles demonstrate that water drains very slowly during the redistribution period, but that this drainage is sustained for tens of thousands of years. If the last glacial period was indeed a time of much greater net infiltration, geochemical evidence of it may exist within water obtained today from the nonwelded and bedded units, with an overprint of more recently infiltrated water.

IV. ASSESSMENT OF MULTIDIMENSIONAL EFFECTS

At this point a few words about the limitations imposed by the dimensionality of our model may be in order. Clearly a one-dimensional model cannot satisfactorily account for the lateral flow components indicated both from tritium data and the analysis of the vertical flux profile. However, vertical and lateral flow are not mutually exclusive and the relative strength of each component cannot be confidently assessed on the basis of the cited data. If the lateral flow component is very strong our conclusions would be changed in the following ways.

First, the inference that the long-term average flux rates have been time-varying may be in error. All that was required to match the observed S and ψ profiles was that fluxes be large in the upper part of the profile and much smaller in the lower part. In a one-dimensional model, this spatial distribution of flux can be achieved only by assuming a time-varying flux. In a multidimensional model, a similar reduction in flux with increasing depth might be achieved through lateral spreading as spatially focussed infiltration encountered layers with varying hydrologic properties. For example, an infiltration flux of 10 mm/yr over a 10 m wide channel may at some depth become a 1 mm/yr flux if in the course of its downward percolation it spreads over an area 100 m wide. While the mechanism that was assumed responsible for the flux reduction at the

base of the nonwelded and bedded interval (a time-varying infiltration rate) may be in part an artifact of the dimensionality assumed by the present model, it is important to note that the basic conclusion of large flux in the upper part of the profile and relatively small flux in the lower part of the profile is not affected by the dimensionality assumed by the model. A large flux on the order of 20 mm/yr is indicated in the upper part of the profile in either case. While the one-dimensional model forces us to conclude that this large flux is a relatively recent transitory phenomena, a two-dimensional model may indicate that this flux represents a relatively constant long-term average.

Secondly, the timing and duration of certain processes and phenomena are also influenced by the assumption of one-dimensional flow. To derive a reasonable match between the observed S and ψ profiles and our simulation results required that we impose an infiltration flux of 20mm/yr for approximately 400 years. If lateral flow had been permitted through the use of a two-dimensional model and infiltration assumed to be concentrated within the wash, this same infiltration flux would need to be imposed for a much greater length of time to reproduce the observed profiles beneath the wash. This is because lateral spreading of water at depth would result in a downward flux that would be less than the imposed flux. We would also expect that for the applied flux of 20 mm/yr, the effectiveness of the capillary barrier at the interface between the nonwelded and bedded tuffs and the fractured, welded tuffs would have been much greater had a two-dimensional model been used. This is because lateral flow along this interface would have further delayed ψ from becoming large enough to initiate fracture flow in the Topopah Spring Member.

Thirdly, during drainage following the imposition of a large flux, we observed that the upper portion of the profile drained comparatively quickly, but in the lower part of the profile, saturations remained high because drainage through the vitric caprock was extremely slow, lasting tens of thousands of years. One might be tempted to say that because S in the lower part of the observed profiles at UZ #4 and UZ #5 are much lower than those predicted for much of the simulated 50,000 year redistribution period, that prior to the most recent period of high infiltration, infiltration beneath the wash had been very low for tens of thousands of years. Again, however, lateral flow may have dissipated the residual buildup in saturation predicted in the lower part of the profile by the one-dimensional simulations, thereby removing such evidence from the observed profiles. Nonetheless, regardless of the dimensionality of the model, it appears that because of capillary barrier effects, water does not readily drain from the nonwelded and bedded intervals and we would expect water that infiltrated even tens of thousands of years ago to be present and mix with more recently infiltrated water.

V. CONCLUSIONS -

The one-dimensional model of water movement beneath Pagany Wash developed in this study has been an important conceptual tool with which to develop hypotheses and, in some cases, provide bounding calculations. Simulation of the measured S and ψ profiles at UZ #4 and UZ #5 has so far suggested the following: (1) Fluxes in the nonwelded base of the Tiva Canyon Member and upper part of the Yucca Mountain Member are relatively large compared with fluxes deeper in the profile, such as those within the upper part of the Topopah Spring Member. Whether the inferred flux reduction with depth has occurred as a result of a time-varying infiltration rate or as a result of areal dispersion of a temporally constant flux with depth can not be established on the basis of a one-dimensional model. (2) Capillary barrier effects should significantly delay any increase in recharge flux associated with future climate change from entering the fractured, densely welded intervals of the Topopah Spring Member. These effects arise due to the contrast in size between pores of the nonwelded tuffs and the apertures of fractures in the underlying welded tuffs. The one-dimensional model used in the present study underestimates the impact of capillary barriers because lateral flow would prolong their effectiveness to an undetermined degree. (3) Even if fractured, the vitric caprock of the Topopah Spring Member should restrict the drainage of water that may have infiltrated into the overlying nonwelded and bedded intervals during past pluvial periods. Because fractures drain quickly, drainage through the matrix of the low-permeability vitric caprock is predicted to be exceedingly slow, causing the ψ profile in the overlying intervals to approach gravity equilibrium in the absence of persistent infiltration or evaporation, or lateral flow. (4) A pronounced asymmetry appears to exist in the time-scales required to wet up the upper unsaturated zone when fracture flow is initiated and to drain this same interval through matrix flow. Due to the slow drainage above the vitric caprock, geochemical evidence of past pluvial periods should persist in the nonwelded and bedded intervals for tens of thousands of years unless obscured by subsequent infiltration.

While the model results indicate that, locally, long-term infiltration rates may be as large as several tens of mm/yr, conclusions (2) and (3) imply that there are features of the natural system at Yucca Mountain that are very effective in delaying the arrival of surface-derived moisture at the proposed repository horizon, thereby making a potentially significant contribution to repository performance.

V. REFERENCES

1. FLINT, A. L., L.E. FLINT, and J.A. HEVESI, "The influence of long-term climate change on net infiltration at Yucca Mountain, Nevada," in *High Level Radioactive Waste Management, Proceedings of the Fourth Annual International Conference*, p. 152-159, American Nuclear Society, La Grange Park, Ill. (1993)

2. WITTWER, C.S., G. CHEN, and G.S. BODVARSSON, "Studies of the role of fault zones on fluid flow using the site-scale numerical model of Yucca Mountain," *in High Level Radioactive Waste Management, Proceedings of the Fourth Annual International Conference*, p. 667-674, American Nuclear Society, La Grange Park, Ill. (1993)

3. KWICKLIS, E.M., A.L. FLINT and R.W. HEALY, "Estimation of unsaturated zone liquid water flow at boreholes UZ #4, UZ #5, UZ #7 and UZ #13, Yucca Mountain, Nevada, from saturation and water potential profiles," *Proceedings of Focus '93, Site Characterization and Model Validation*, Sept. 26-29, Las Vegas, American Nuclear Society, La Grange Park, Ill. (1994)

4. LOSKOT, C.L. and HAMMERMEISTER, D.P., "Geohydrologic data from test holes UE-25 UZ #4 and UE-25 UZ #5, Yucca Mountain area, Nye County, Nevada," *U. S. Geological Survey Open-File Report 90-369*, 56 p. (1992)

5. VAN GENUCHTEN, M. TH., "A closed-form equation for predicting hydraulic conductivity of unsaturated soils," *Soil Sci. Soc. Am. J.*, 44, p. 892-898. (1980)

6. YANG, I.C., "Flow and transport through unsaturated rock - data from two test holes, Yucca Mountain, Nevada," in *High Level Radioactive Waste Management, Proceedings of the Third International Conference*, p. 732-737, American Nuclear Society, La Grange Park, Ill. (1992)

7. HEVESI, J.A. and A.L. FLINT, "The influence of seasonal climatic variability on shallow infiltration at Yucca Mountain," *High-Level Radioactive Waste Management, Proceedings of the Fourth Annual International Conference*, p. 122-131, American Nuclear Society, La Grange Park, Ill. (1993)

8. SCOTT, R.B. and J. BONK, "Preliminary geologic map of Yucca Mountain, Nye County, Nevada, with geologic sections", *U.S. Geologic Survey Open File Report 84-494*, 9 p. (1984)

9. SCOTT, R.B., R.W. SPENGLER, S.DIEHL, A.R. LAPPIN, AND M.P. CHORNACK, "Geologic character of tuffs in the unsaturated zone at Yucca Mountain, southern Nevada," in *Role of the unsaturated zone in radioactive and hazardous waste disposal*, Ann Arbor Science, Butterworth Group, p. 289-335. (1983)

10. KWICKLIS, E.M. and R. W. HEALY, "Numerical investigation of steady liquid water flow in a variably saturated fracture network," *Water Resources Research*, v. 29, no. 12, p. 4091-4102. (1993)

11. PRUESS, K., "TOUGH User's Guide," *Report LBL-20700*, Lawrence Berkely Laboratory, Berkeley, CA, 78 p. (1987)

DISCLAIMER

HIGH LEVEL RADIOACTIVE WASTE MANAGEMENT

Proceedings of the Fifth Annual International Conference
Las Vegas, Nevada, May 22-26, 1994

VOLUME 4
1994

Sponsored by the
American Society of Civil Engineers
American Nuclear Society

in cooperation with:

American Association of Engineering Societies
American Chemical Society
American Institute of Chemical Engineers
American Medical Association
American Society for Testing and Materials
American Society for Quality Control
American Society of Mechanical Engineers
Center for Nuclear Waste Regulatory Analysis
Edison Electric Institute
Geological Society of America
Health Physics Society
Institute of Nuclear Materials Management
National Conference of State Legislatures
Society of Mining Engineers
U.S. Department of Energy
U.S. Geological Survey
U.S. Nuclear Regulatory Commission
University of Nevada Medical School
American Institute of Mining, Metallurgical and Petroleum Engineers
American Underground-Space Association
Atomic Energy Council Radwaste Administration
Atomic Energy of Canada Ltd.
British Nuclear Fuels Ltd.
Chinese Institute of Civil and Hydraulic Engineering
Commission of the European Communities
Conseil National des Ingenieurs et des Scientifiques de France
Electric Power Research Institute
Her Majesty's Inspectorate of Pollution
Hungarian Nuclear Society
Institution of Civil Engineers
Institution of Engineers-Australia
Institution of Engineers of Ireland
Japan Society of Civil Engineers
Korea Advanced Energy Research Institute
Korean Society of Civil Engineers
Ministerio de Industria y Energia-Uruguay
National Association of Corrosion Engineers
National Association of Regulatory Utility Commissioners
Nationale Genossenschaft fur die Lagerung Radioaktiver Abfalle (NAGRA)
National Society of Professional Engineers
Organization for Economic Cooperation and Development (OECD)- Nuclear Energy Agency
Power Reactor and Nuclear Fuel Development Corp.
Romanian Nuclear Energy Association
Swedish Nuclear Fuel and Waste Management Company
Swedish Nuclear Power Inspectorate
Swiss Society of Engineers and Architects
U.S. Council for Energy Awareness
Verein Deutscher Ingenieure

Hosted by
University of Nevada, Las Vegas
Howard R. Hughes College of Engineering

Published by the

American Nuclear Society, Inc.
La Grange Park, Illinois 60525, USA

American Society of Civil Engineers
345 East 47th Street
New York, New York 10017-2398, USA